Institut für Mathematik

Optimization of a thermal coupled flow problem part I: Algorithms and numerical results

Günter Bärwolff Michael Hinze

Preprint 15-03

Preprint-Reihe des Instituts für Mathematik
Technische Universität Berlin

Report 15-03 July 2003

Optimization of a thermal coupled flow problem part I: Algorithms and numerical results

Günter Bärwolff[1] and Michael Hinze[2]

[1] TU Berlin, Institute of Mathematics, D-10623 Berlin, Str. d. 17. Juni 135, Germany
[2] TU Dresden, Institute of Mathematics, D-01062 Dresden, Zellescher Weg 12-14, Germany

1 Introduction

During the growth of crystals crystal defects were observed under some conditions of the growth device. A transition from the twodimensional flow regime of a crystal melt in axisymmetric zone melting devices to an unsteady threedimensional behavior of the velocity and temperature field was found experimentally. This behavior leads to striations as undesirable crystal defects. To avoid such crystal defects it is important to know the parameters, which guarantee a stable steady twodimensional melt flow during the growth process.
There are several possibilities for parameter finding. In this paper optimization problems will be discussed. From the experiment and the practical crystal production process it is known that an unsteady behavior of the melt and vorticies near the fluid-solid-interphase decrease the crystal quality. Thus it makes sense to look for example for

(i) flows, which are nearly steady and
(ii) flows, which have only a small vorticity in a certain region of the melt zone.

This leads to tracking type optimization problems (i) with functionals like

$$J(\boldsymbol{u},\theta_c) = \frac{1}{2}\int_0^T \int_\Omega |\boldsymbol{u}-\overline{\boldsymbol{u}}|^2 \, d\Omega dt + \frac{\alpha}{2}\int_0^T \int_{\Gamma_c} (\theta_c^2 + \theta_{c_t}^2) \, d\Omega dt \tag{1}$$

and problems with optimization functionals of the form

$$J(\boldsymbol{u},\theta_c) = \frac{1}{2}\int_0^T \int_\Omega |curl\boldsymbol{u}|^2 \, d\Omega dt + \frac{\alpha}{2}\int_0^T \int_{\Gamma_c} \theta_c^2 \, d\Omega dt \; . \tag{2}$$

$\boldsymbol{u}$ is the velocity vector field in the melt and $\overline{\boldsymbol{u}}$ is the state, which we want to have, θ_c is the control temperature on the control boundary Γ_c. The discussed methods of deriving optimization and the iterative algorithms of the evaluation of necessary optimality conditions are investigated by the solution of typical crystal growth problems. Because of the difficulties to construct or to prescribe desirable flow fields we use $\overline{\boldsymbol{u}}$ which we got by a certain forward solution of the Boussinesq equation system or we set $\overline{\boldsymbol{u}}$ equal to zero. But with the optimization strategy we are ready to compute an optimal control for a given desirable flow field $\overline{\boldsymbol{u}}$ by crystal growth engineers.

2 Mathematical model

The crystal melt is described by the Navier-Stokes equation for an incompressible fluid using the Boussinesq approximation coupled with the convective heat conduction equation and the diffusion equation. Heat conductivity and viscosity depend on the temperature. Because of the axisymmetric situation of the melting zone we write down the equations in cylindrical coordinates. Thus we have a Boussinesq equation system in cylindrical coordinates for the velocity $\boldsymbol{u} = (u, v, w)$, the pressure p and the temperature θ.

$$u_t + (ruu)_r/r + (uv)_\varphi/r + (wu)_z - v^2/r = \qquad (3)$$
$$- p_r + ((ru)_r/r)_r + u_{\varphi\varphi}/r^2 - 2v_\varphi/r^2 + u_{zz}\,,$$
$$v_t + (ruv)_r/r + (vv)_\varphi/r + (wv)_z + uv/r = \qquad (4)$$
$$- p_\varphi/r + \; ((rv)_r/r)_r + v_{\varphi\varphi}/r^2 + 2u_\varphi/r^2 + v_{zz}\,,$$
$$w_t + (ruw)_r/r + (vw)_\varphi/r + (ww)_z = \qquad (5)$$
$$- p_z + (rw_r)_r/r + w_{\varphi\varphi}/r^2 + w_{zz} + Gr\,\theta\,,$$
$$(ru)_r/r + v_\varphi/r + w_z = 0\,, \qquad (6)$$
$$\theta_t + (ru\theta)_r/r + (v\theta)_\varphi/r + (w\theta)_z = \frac{1}{Pr}[(r\theta_r)_r/r + (\theta_\varphi)_\varphi/r^2 + (\theta_z)_z] + f\ , \quad (7)$$

in the cylindrical melt zone (height H, radius R). u, v, w and p are the primitive variables of the velocity vector and the pressure, ρ and θ denote the density and the temperature, Gr is the Grashof number, Pr is the Prandtl number, and f stands for an energy source.
For the velocity no slip boundary conditions are used. At the interfaces between the solid material and the fluid crystal melt we have for the temperature inhomogenous Dirichlet data, i.e. the melting point temperature. The boundary conditions are of the form

$$u = u_d \quad \text{and} \quad v = w = 0 \quad \text{on the whole boudary,} \qquad (8)$$
$$\theta = \theta_c \quad \text{for } r = R, 0 \le z \le H, \varphi \in (0, 2\pi),\ \text{(control boundary } \Gamma_c), \qquad (9)$$
$$\theta = \theta_d, \quad \text{for } 0 \le r \le R, z = 0,\ z = H, \varphi \in (0, 2\pi). \qquad (10)$$

In the case of the Czochralski crystal growth technique with u_d we have the possibility to describe a certain crystal and crucible rotation. In the case of zone melting flow u_d equals zero. The initial state was assumed as the neutral position of the crystal melt ($\boldsymbol{v} = \boldsymbol{0}$) and a temperature field, which solves the non convective heat conduction equation with the given temperature boundary conditions.
The material properties and the dimensionless parameters for the investigated crystal close the initial boundary value problem for the description of the melt flow.

3 Optimization

For the calculus of optimization and the derivation of an optimization system we use the following dimesionless mathematical model in cartesian coordinates, which reads as

$$\boldsymbol{u}_t + (\boldsymbol{u}\cdot\nabla)\boldsymbol{u} - \Delta\boldsymbol{u} + \nabla p - Gr\,\theta\,\boldsymbol{g} = 0 \quad \text{on } \Omega_T, \tag{11}$$

$$-div\;\boldsymbol{u} = 0 \quad \text{on } \Omega_T, \tag{12}$$

$$\theta_t + (\boldsymbol{u}\cdot\nabla)\theta - \frac{1}{Pr}\Delta\theta - f = 0 \quad \text{on } \Omega_T \;. \tag{13}$$

The vector $\boldsymbol{g}$ is directed in the z-direction, i.e. $\boldsymbol{g} = (0,0,1)$. We will now discuss the case $f = 0$. $\boldsymbol{u}$ is the velocity vector and $\Omega_T = \Omega \times (0,T)$ is the considered time cylinder. For the boundary conditions we have

$$\boldsymbol{u} = \boldsymbol{u}_d \quad \text{on } \Gamma \times (0,T), \quad \theta = \theta_c \ \text{ on } \Gamma_{cT}, \ \text{ and } \quad \theta = \theta_d \ \text{ on } \Gamma_d \times (0,T), \tag{14}$$

where Γ is the boundary of the spatial region $\Omega \subset \mathbb{R}^3$, on which the problem lives, and Γ_c is the control boundary, Γ_d is the Dirichlet part of the boundary and $\Gamma_{cT} = \Gamma_c \times (0,T)$. For $t = 0$ we have the initial condition $\boldsymbol{u} = \boldsymbol{0}$ and a temperature field, which solves the non convective heat conduction equation with the given temperature boundary conditions $\theta = \theta_0$ on Ω.
The use of formal Lagrange parameter technique with respect to the functional of type (1) means the consideration of the Lagrange functional

$$\begin{aligned} L(\boldsymbol{u},p,\theta,\theta_c,\boldsymbol{\mu},\xi,\kappa,\chi) &= J(\boldsymbol{u},\theta_c) + <\boldsymbol{\mu}, mo>_{\Omega_T} \\ &- <\xi, div\,\boldsymbol{u}>_{\Omega_T} + <\kappa, en>_{\Omega_T} + <\chi, \theta-\theta_c>_{\Gamma_{cT}} \;. \end{aligned} \tag{15}$$

mo and en stand for the left sides of the equations (11) and (13), and for example for $<\boldsymbol{\mu}, mo>_{\Omega_T}$ we have

$$<\boldsymbol{\mu}, mo>_{\Omega_T} = \int_{\Omega_T} [\boldsymbol{u}_t + (\boldsymbol{u}\cdot\nabla)\boldsymbol{u} - \Delta\boldsymbol{u} + \nabla p - Gr\,\theta\,\boldsymbol{g}]\cdot\boldsymbol{\mu}\, d\Omega\, dt \;. \tag{16}$$

$\boldsymbol{\mu}$, ξ, κ and χ are Lagrange parameters. We will not discuss the functional analytical aspects of the used Lagrange method, i.e. function spaces, smoothness properties etc. in detail. A very good overview over the functional analytical background and the foundation of the optimization of Navier-Stokes problems is developed in [2].
To find candidates $\boldsymbol{u}(\theta_c)$ and θ_c, which minimize the functional (1) we have to analyze the necessary conditions

$$\begin{aligned} L_{\boldsymbol{u}}\tilde{u} &= J_{\boldsymbol{u}}\tilde{u} \qquad\qquad (17) \\ &\quad + <\boldsymbol{\mu}, mo_{\boldsymbol{u}}>_{\Omega_T} - <\xi, div\tilde{u}>_{\Omega_T} + <\kappa, en_{\boldsymbol{u}}>_{\Omega_T} = 0, \\ L_p\tilde{p} &= <\nabla\tilde{p}, \boldsymbol{\mu}>_{\Omega_T} = 0, \qquad\qquad (18) \\ L_\theta\tilde{\theta} &= <-Gr\,\boldsymbol{g}\,\tilde{\theta}, \boldsymbol{\mu}>_{\Omega_T} + <\kappa, en_\theta>_{\Omega_T} + <\chi, \tilde{\theta}>_{\Gamma_{cT}} = 0, \qquad (19) \\ L_{\theta_c}\tilde{\theta}_c &= J_{\theta_c}\tilde{\theta}_c + <-\chi, \tilde{\theta}_c>_{\Gamma_{cT}} = 0 \;. \qquad\qquad (20) \end{aligned}$$

Let us have a closer look at the condition (17). For $J_{\boldsymbol{u}}\tilde{u}$ we find

$$J_{\boldsymbol{u}}\tilde{u} = \int_{\Omega_T} (\boldsymbol{u} - \overline{\boldsymbol{u}}) \cdot \tilde{u} \, d\Omega dt \; . \tag{21}$$

The term $< \boldsymbol{\mu}, mo_{\boldsymbol{u}} >_{\Omega_T}$ means the derivative of the Navier-Stokes equation, i.e.

$$< \boldsymbol{\mu}, mo_{\boldsymbol{u}} >_{\Omega_T} = \int_{\Omega_T} [\tilde{u}_t - \Delta\tilde{u} + (\boldsymbol{u} \cdot \nabla)\tilde{u} + (\tilde{u} \cdot \nabla)\boldsymbol{u}] \cdot \boldsymbol{\mu} \, d\Omega dt \; . \tag{22}$$

The discussion of the term $< \kappa, en_{\boldsymbol{u}} >_{\Omega_T}$ gives

$$< \kappa, en_{\boldsymbol{u}} >_{\Omega_T} = \int_{\Omega_T} [(\tilde{u} \cdot \nabla)\theta]\kappa \, d\Omega dt \; . \tag{23}$$

Using the rules of integration by parts from (21)-(23) and (17) we get for all test vector functions $\tilde{u}$

$$L_{\boldsymbol{u}}\tilde{u} = \int_{\Omega_T} [-\boldsymbol{\mu}_t - \Delta\boldsymbol{\mu} + (\nabla\boldsymbol{u})^t\boldsymbol{\mu} - (\boldsymbol{u} \cdot \nabla)\boldsymbol{\mu} + \nabla\xi + (\boldsymbol{u} - \overline{\boldsymbol{u}}) + \kappa\nabla\theta] \cdot \tilde{u} \, d\Omega dt = 0 \; ,$$

or

$$-\boldsymbol{\mu}_t - \Delta\boldsymbol{\mu} + (\nabla\boldsymbol{u})^t\boldsymbol{\mu} - (\boldsymbol{u} \cdot \nabla)\boldsymbol{\mu} + \nabla\xi = -(\boldsymbol{u} - \overline{\boldsymbol{u}}) - \kappa\nabla\theta \quad \text{in} \quad \Omega_T \; , \tag{24}$$

with the boundary condition and the final condition

$$\boldsymbol{\mu} = \mathbf{0} \quad \text{on} \quad \Gamma \times (0,T), \quad \text{and} \quad \boldsymbol{\mu}(T) = \mathbf{0} \quad \text{in} \quad \Omega \; . \tag{25}$$

The necessary condition (18) gives for all test functions $\tilde{p}$ the equation

$$-div \; \boldsymbol{\mu} = 0 \quad \text{in} \quad \Omega_T \; . \tag{26}$$

The condition (19) means

$$\begin{aligned} L_\theta\tilde{\theta} = & \int_{\Omega_T} -Gr \, \boldsymbol{g} \cdot \boldsymbol{\mu} \, \tilde{\theta} \, d\Omega dt \\ & + \int_{\Omega_T} [\tilde{\theta}_t - \frac{1}{Pr}\Delta\tilde{\theta} + \boldsymbol{u} \cdot \nabla\tilde{\theta}]\kappa \, d\Omega dt + \int_{\Gamma_{cT}} \chi\tilde{\theta} \, d\Gamma_c dt = 0 \; , \end{aligned}$$

or after the integration by parts for all test functions $\tilde{\theta}$ we get the equation

$$-\kappa_t - \frac{1}{Pr}\Delta\kappa - (\boldsymbol{u} \cdot \nabla)\kappa = Gr \, \boldsymbol{g} \cdot \boldsymbol{\mu} \quad \text{in} \quad \Omega_T \; , \tag{27}$$

with the boundary condition and the final condition

$$\kappa = 0 \quad \text{on} \quad \Gamma \times (0,T), \quad \text{and} \quad \kappa(T) = 0 \quad \text{in} \quad \Omega \; , \tag{28}$$

and the choice of χ as

$$\chi = -\frac{1}{Pr}\frac{\partial\kappa}{\partial\mathbf{n}} \quad \text{on} \quad \Gamma_{cT} \; .$$

The evaluation of the condition (20) finally gives

$$\alpha(-\theta_{c_{tt}} + \theta_c) = \chi \; (= -\frac{1}{Pr}\frac{\partial\kappa}{\partial\mathbf{n}}) \quad \text{on} \quad \Gamma_{cT} \; , \tag{29}$$

with the time boundary conditions

$$\theta_c(0) = \theta_0 \quad \text{and} \quad \theta_{c_t}(T) = 0 \; , \tag{30}$$

where θ_0 means a temperature distribution on Γ_c at the beginning of the melting process. Now we can summarize, and the fully optimization system consists of

- the forward model with the Boussinesq equations (11),(12),(13), the boundary condition (14) and the given initial state for the velocity field $\boldsymbol{u}$, the pressure p and the temperature θ, and
- the adjoint model with the equations (24),(26),(27),(29), and the conditions (25),(28),(30) for the adjoint variables $\boldsymbol{\mu}$, ξ, κ and the control θ_c,

and we will call it optimization system (I). The global existence of a solution of the forward problem is well known (see [4], [5]). In three dimensions only the local uniqueness of the forward solution could be shown. Hinze [2] has shown the existence and uniqueness of a solution of the adjoint model. Minimization functionals of the considered types (1) are investigated by Hinze [2], and the discussion of qualitative questions like existence of a minimum of

$$\hat{J}(\theta_c) := J(\boldsymbol{u}(\theta_c), \theta_c) \; ,$$

will be done later.
Now we will discuss the question, do we have enough smoothness of our control to work with the functional

$$J(\boldsymbol{u}, \theta_c) = \frac{1}{2}\int_0^T \int_\Omega |\boldsymbol{u} - \overline{\boldsymbol{u}}|^2 \, d\Omega dt + \frac{\alpha}{2}\int_0^T \int_{\Gamma_c} (\theta_c^2 + \theta_{c_t}^2) \, d\Omega dt$$

and the resulting two point boundary value problem

$$\alpha(-\theta_{c_{tt}} + \theta_c) = -\frac{1}{Pr}\frac{\partial\kappa}{\partial\mathbf{n}} \quad \text{on} \quad \Gamma_c \times (0,T) \; , \quad \theta_c(0) = \theta_0 \quad \text{and} \quad \theta_{c_t}(T) = 0 \; ?$$

Instead of the functional (1) we can use

$$J(\boldsymbol{u}, \theta_c) = \frac{1}{2}\int_0^T \int_\Omega |\boldsymbol{u} - \overline{\boldsymbol{u}}|^2 \, d\Omega dt + \frac{\alpha}{2}\int_0^T \int_{\Gamma_c} (\theta_c^2 + \eta^2) \, d\Omega dt \, , \tag{31}$$

and in addition to our Boussinesq equation system the ordinary differential equation

$$\theta_{c_t} = \eta \;\; \text{on} \;\; \Gamma_{cT} \; . \tag{32}$$

Initial conditions will be considered later. With the new equation (32) we need one more Lagrange parameter and the Lagrange function reads

$$\begin{aligned} &L(\boldsymbol{u}, p, \theta, \theta_c, \boldsymbol{\mu}, \xi, \kappa, \chi, \zeta) = J(\boldsymbol{u}, \theta_c, \eta) + < \boldsymbol{\mu}, mo >_{\Omega_T} \\ &\quad - < \xi, div\, \boldsymbol{u} >_{\Omega_T} + < \kappa, en >_{\Omega_T} + < \chi, \theta - \theta_c >_{\Gamma_{cT}} + < \zeta, \theta_{c_t} - \eta >_{\Gamma_{cT}} \; . \end{aligned}$$

Now we will analyze the derivatives of L over θ_c and η. We find

$$L_{\theta_c}\tilde{\theta}_c = J_{\theta_c}\tilde{\theta}_c + < -\chi, \tilde{\theta}_c >_{\Gamma_{cT}} + < \zeta, \tilde{\theta}_{c_t} >= 0 \tag{33}$$

$$L_\eta\tilde{\eta} \quad = J_\eta\tilde{\eta} + < \zeta, -\tilde{\eta} >_{\Gamma_{cT}} = 0 \; . \tag{34}$$

The discussion of the equation (33) gives after integration by parts

$$\alpha\theta_c - \chi = \zeta_t, \;\text{ with }\; \zeta(T) = 0 \; . \tag{35}$$

From equation (34) we have

$$\zeta = \alpha\eta \quad \text{or} \quad \zeta = \alpha\theta_{c_t} \; . \tag{36}$$

That means in the case of the functional (31) we have to solve the ode system

$$\theta_{c_t} = \frac{1}{\alpha}\zeta, \quad \theta_c(0) = \theta_0 \quad \text{on } \Gamma_{cT} \tag{37}$$

$$-\zeta_t = -\alpha\theta_c + \chi, \quad \zeta(T) = 0 \quad \text{on } \Gamma_{cT} \; , \tag{38}$$

instead of the two point boundary value problem (29),(30) for the functional (1). For the functional (31) we can summarize the fully optimization system and we get

- the forward model with the Boussinesq equations (11),(12),(13), the boundary condition (14) and the given initial state for the velocity field $\boldsymbol{u}$, the pressure p and the temperature θ, and
- the adjoint model with the equations (24),(26),(27),(37),(38), and the conditions (25),(28) for the adjoint variables $\boldsymbol{\mu}$, ξ, κ , ζ and the control θ_c,

and we will call it optimization system (II). It is easy to see, that if we have enough smoothness of our control θ_c the ode system (37),(38) is equivalent to the two point boundary value problem (29),(30).

4 Optimization with infinite degrees of freedom vs. optimization of finite parameters

In our concept we look for a boundary control θ_c, which has infinite degrees of freedom. The prize we have to pay for this is high, because of the very complicated optimization system consisting of the forward and the adjoint system, which is hard to solve. Other concepts (for example [6]) look for special control functions, which only depend on a few parameters (in [6] are two parameters used). This restriction gives the possibility to minimize a given functional in the case of two parameters by a Newton method, and for one Newton iteration the forward problem must be solved three times.
Because of the more general concept a result θ_c of the presented optimization strategy will be optimal in a more general sense, than prescribed temperature profiles, which only depend on two parameters. But the easier implementation of the method, presented in [6], makes it to a valuable optimization tool.

5 To the numerical solution method of the full problem

The optimization system (I) is now under consideration for a numerical solution. The used time discretization should be demonstrated for the forward problem (11)-(14), i.e. the boussinesq equation system. The adjoint problem will be treated in a similar way. Quantities without upper indices are considered at the old time level $t_n = n\tau$ with the time step τ. The upper index $n+1$ means the values at the new time level $t_{n+1} = (n+1)\tau$. With $\tau = \frac{T}{Z}$ we have a discretization $t_0 = 0$, $t_1 = \tau$, $t_2 = 2\tau, \ldots, t_Z = Z\tau = T$ of the considered time intervall $[0, T]$. We use an implicit time discretization related to the conductive terms controlled by the weighting parameters σ_m, σ_h $\in]0, 1]$. Thus we have the time integration scheme

$$\begin{aligned} &\frac{\boldsymbol{u}^{n+1} - \boldsymbol{u}}{\tau} + (\boldsymbol{u} \cdot \nabla)\boldsymbol{u} - \Delta(\sigma_m \boldsymbol{u} + (1-\sigma_m)\boldsymbol{u}^{n+1}) \\ &\qquad\qquad + \nabla(\sigma_m p + (1-\sigma_m)p^{n+1}) - Gr\,\theta^{n+1}\boldsymbol{g} = 0 \quad \text{on } \Omega_T \qquad (39) \\ &-div\ \boldsymbol{u}^{n+1} = 0 \quad \text{on } \Omega_T \qquad (40) \\ &\frac{\theta^{n+1} - \theta}{\tau} + (\boldsymbol{u} \cdot \nabla)\theta - \frac{1}{Pr}\Delta(\sigma_h \theta + (1-\sigma_h)\theta^{n+1}) = 0 \quad \text{on } \Omega_T \ . \qquad (41) \end{aligned}$$

The divergence of the equation (39) gives

$$-(1-\sigma_m)\Delta p^{n+1} = -\frac{1}{\tau} div\ \tilde{\boldsymbol{u}} \quad , \tag{42}$$

with

$$\tilde{\boldsymbol{u}} = \boldsymbol{u} + \tau[(\boldsymbol{u} \cdot \nabla)\boldsymbol{u} - \sigma_m \Delta \boldsymbol{u} + \sigma_m \nabla p + Gr\,\theta^{n+1}\boldsymbol{g}] \ . \tag{43}$$

With the solution p^{n+1} of the equation (42) the velocity field $\boldsymbol{u}^{n+1}$ we get as the solution of

$$\frac{1}{\tau}\boldsymbol{u}^{n+1} - (1-\sigma_m)\Delta \boldsymbol{u}^{n+1} = \frac{1}{\tau}\boldsymbol{u} - (1-\sigma_m)\nabla p^{n+1} \quad . \tag{44}$$

The used time discretization means the solution of a Poisson equation for p^{n+1}, four Helmholtz equations for the components of $\boldsymbol{u}^{n+1}$ and θ^{n+1}. The spatial finite volume discretization developed in [1] of the equations (42), (44) and (41) leads to linear equation systems with symmetric coefficient matrices which we solve with conjugate gradient methods. The same time discretization is used for the adjoint problem.

Now we discuss some aspects of our special axisymmetric case. If we have axisymmetric conditions we can transform the adjoint equations into a cylindrical coordinate system. Using the adjoint divergence condition $div\, \boldsymbol{\mu} = 0$ we can write the adjoint equations in the following quasi conservative form. For the adjoint velocity $\boldsymbol{\mu} = (\mu, \nu, \omega)$ in the cylindrical coordinate system with the radial component μ, the azimutal component ν and the z-component ω using the adjoint divergence condition $div\, \boldsymbol{\mu} = 0$ we can write the adjoint equations (24) in the following quasi conservative form.

$$-\mu_t - ((r\mu)_r/r)_r - \mu_{\varphi\varphi}/r^2 + 2\mu_\varphi/r^2 - \mu_{zz} + \mu u_r + \nu v_r + \omega w_r \qquad (45)$$
$$-(ru\mu)_r/r - (v\mu)_\varphi/r - (w\mu)_z + v\nu/r + \xi_r = -(u-\overline{u}) - \kappa\theta_r$$
$$-\nu_t - ((r\nu)_r/r)_r - \nu_{\varphi\varphi}/r^2 - 2\nu_\varphi/r^2 - \nu_{zz} \qquad (46)$$
$$+\mu u_\varphi/r + \nu v_\varphi/r + \omega w_\varphi/r + (\nu u - \mu v)/r$$
$$-(ru\nu)_r/r + (v\nu)_\varphi/r - v\mu/r - (w\nu)_z + \xi_\varphi/r = -(v-\overline{v}) - \kappa\theta_\varphi/r$$
$$-\omega_t - (r\omega_r)_r/r - \omega_{\varphi\varphi}/r^2 - \omega_{zz} + \mu u_z + \nu v_z + \omega w_z \qquad (47)$$
$$-(ru\omega)_r/r - (v\omega)_\varphi/r - (w\omega)_z + \xi_z = -(w-\overline{w}) - \kappa\theta_z \ .$$

From equation (27) we get for the adjoint temperature κ

$$-\kappa_t - \frac{1}{Pr}[(r\kappa_r)_r/r + \kappa_{\varphi\varphi}/r^2 + \kappa_{zz}] - (ru\kappa)_r/r - (v\kappa)_\varphi/r - (w\kappa)_z = Gr\,\omega \ . \quad (48)$$

Equation (48) is a convective heat conduction equation and the discretization can be done like those in [1]. In the equations (45)-(47) the terms

$$(\nabla \boldsymbol{u})^t \boldsymbol{\mu} \qquad \text{and} \qquad \kappa\nabla\theta$$

are not known from the classical Navier-Stokes equations. Using a staggered grid finite volume method, u and μ live at the same gridpoints, also v and ν, w and ω, and θ and κ. Let us discuss the first component of $(\nabla \boldsymbol{u})^t \boldsymbol{\mu}$ and $\kappa\nabla\theta$, we get in a canonical way

$$(\mu u_r + \nu v_r + \omega w_r)_{i+1/2jk} \approx \qquad (49)$$
$$\mu_{i+1/2jk}[(u_{i+3/2jk} + u_{i+1/2jk}) - (u_{i+1/2jk} + u_{i-1/2jk})]/(2\Delta x_{i+1/2})$$
$$+\nu_{i+1/2jk}[(v_{i+1j+1/2k} + v_{i+1j-1/2k}) - (v_{ij+1/2k} + v_{ij-1/2k})]/(2\Delta x_{i+1/2})$$
$$+\omega_{i+1/2jk}[(w_{i+1jk+1/2} + w_{i+1jk-1/2}) - (w_{ijk+1/2} + w_{ijk-1/2})]/(2\Delta x_{i+1/2})$$

with

$$\nu_{i+1/2jk} = (\nu_{ij+1/2k} + \nu_{i+1j+1/2k} + \nu_{ij-1/2k} + \nu_{i+1j-1/2k})/4 \quad \text{and}$$

$$\omega_{i+1/2jk} = (\omega_{i+1jk+1/2} + \omega_{i+1jk-1/2} + \omega_{ijk+1/2} + \omega_{ijk-1/2})/4 \ ,$$

and

$$\kappa\theta_r \approx 0.5(\kappa_{i+1jk} + \kappa_{ijk})[\theta_{i+1jk} - \theta_{ijk}]/\Delta x_{i+1/2} \ . \qquad (50)$$

For the control θ_c we got the equation (29)

$$-\theta_{c_{tt}} + \theta_c = \chi \, (= -\frac{1}{\alpha Pr}\frac{\partial\kappa}{\partial \mathbf{n}}) \quad \text{on} \quad \Gamma_{cT},$$

with the boundary conditions $\theta_c(\gamma, 0) = \theta_{c0}$ and $\theta_{c_t}(\gamma, T) = 0$ for $\gamma \in \Gamma_c$. The numerical solution of this two point boundary value problem is done with a finite

volume method in space and time.
The solution of the discretized system (11)-(14) and (24)-(30) is difficult and expensive, because of the opposite time direction of the forward system (11)-(14) and the adjoint system (24)-(30). That means we know the forward solution $\boldsymbol{u}, \theta$ on the whole time interval $[0, T]$ to get the adjoint solution $\boldsymbol{\mu}, \kappa, \theta_c$ and vice versa.
If we have discretized the time interval $[0, T]$ by Z timesteps $\tau = \frac{1}{Z}$ and the dimensions of the spatial discretizations are N, M and P a direct solution of the whole system means the solution of an algebraic equation system with $2Z \times N \times M \times P \times 10$ equations. For the representation of the used iteration method we denote with $\mathcal{H} := -\partial_{tt} + id$ an invertible operator, which describes the solution of the two point boundary value problem (29),(30) on Γ_{cT}, i.e.

$$\mathcal{H}(\theta_c) = \chi \quad \text{or} \quad \theta_c = \mathcal{H}^{-1}(\chi) \; .$$

Iterative methods of the form

i) choose a suitable start value of θ_c,
ii) solve the forward problem and get $[\boldsymbol{u}, \theta](\theta_c)$
iii) solve the adjoint problem and get $[\boldsymbol{\mu}, \kappa](\boldsymbol{u}, \theta)$
update of θ_c by $\theta_c := \sigma_r \theta_c + (1 - \sigma_r)\mathcal{H}^{-1}(\chi)$, $\sigma_r \in]0, 1[$,
iv) until convergence, go to ii),

are used. In the case of the optimization system (II) we have to solve the ode system (37),(38) instead of the two point boundary value problem (29),(30). We do this by

$$\frac{\theta_c^{n+1} - \theta_c^n}{\tau} = \frac{1}{\alpha} \zeta^{n+1}, \; n = 0, \ldots, Z-1 \, , \theta^0 = \theta_0 \; , \tag{51}$$

$$-\frac{\zeta^{n+1} - \zeta^n}{\tau} = -\alpha \theta_c^n + \chi^n, \; n = Z-1, \ldots, 0 \; \zeta^Z = 0 \; . \tag{52}$$

The combination of (51) and (52) gives with

$$-\frac{\theta_c^{n+1} - 2\theta_c^n + \theta_c^{n-1}}{\tau^2} + \theta_c^n = \frac{1}{\alpha} \chi^n, \; n = 1, \ldots, Z-1, \; \theta^0 = \theta_0, \; \frac{\theta_c^Z - \theta_c^{Z-1}}{\tau} = 0 \; , \tag{53}$$

a numerical solution method of (29),(30). That means in the case of the convergence of the fixpoint iteration for the full problem the solution of the optimization system (I) is a solution of (II) and vice versa. We controlled this fact by the implementation of the two methods and found equal solutions in both cases.
During one time step of the forward problem we have to solve equations of the type (42), a Poisson equation, and with (44),(41) four Helmholtz equations (for the adjoint problem also five equations of the same type). We do this with a preconditioned conjugate gradient method.
The above described fixpoint iteration i)-iv) with relaxation works good, and the results of the numerical simulations will be demonstrated now.

6 Results of the numerical solution of the full problem

As a first testproblem we consider an idealized Czochralski crystal growth process. The figure 1 shows the geometrical situation of the crucible. The above

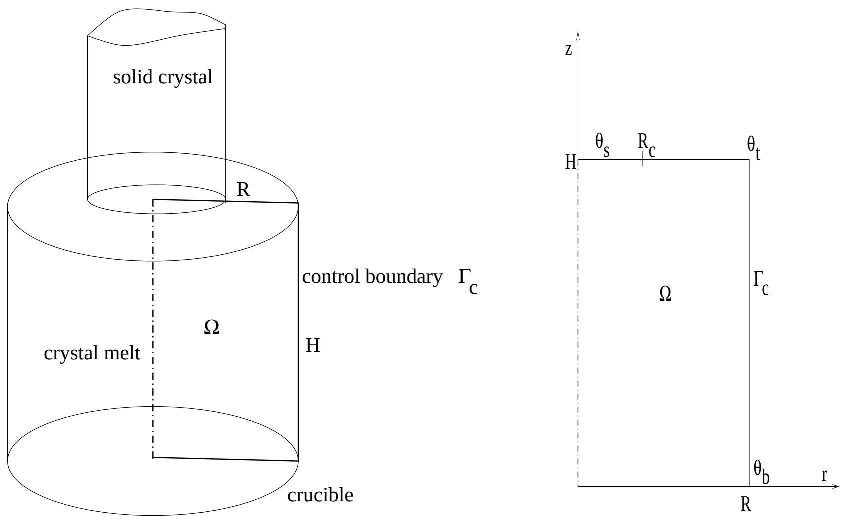

Fig. 1. Physical domain for Czochralski growth

discussed model and the optimization system is formulated and implemented in three dimensions. Because of the huge computational amount we test the optimization procedure for the twodimensional case $u = 0$ (azimuthal component of the velocity) and $\frac{\partial Q}{\partial \varphi} = 0$ for all transport quantities Q ($\boldsymbol{u}, p, \theta$, etc.). Thus we have a twodimensional integration region (see figure 1). R_c is the radius of the solid crystal, R is the crucible radius and H is the height of the crystal melt. θ_s is the melting point temperature of the crystal material, θ_b and θ_t are temperatures with $\theta_b > \theta_t > \theta_s$. In the table 1 the used geometrical and material parameters for a Silicium Czochralski growth process found in [8] are summarized.

parameter	symbol	value
crucible radius	R	0.15 m
crystal radius	R_c	0.075 m
height of the melt	H	0.4 m
melting point temperatur	θ_s	1683 K
thermal diffusivity	a	0.264e-04 $\frac{m^2}{s}$
kinematic viscosity	ν	0.279e-06 $\frac{m^2}{s}$
thermal expansion coefficient	β	1.41*10^{-4} K^{-1}

Table 1. Parameters of Silicium and of the melt geometry

The material parameters give a Grashof number of $1.5e+09$ and this magnitude leads to a strong CFL restriction for the used time discretization. It's only possible to work with time steps of $\tau \approx 10e-05$. But it is not so strong than it seems. One dimensionless time step $\tau = 10e-05$ is equal to a time of 0.80645 seconds. For the thermal boundary conditions of our Czochralski process we have

$$\theta = \theta_c \quad \text{for } r = R, 0 \le z \le H, \varphi \in (0, 2\pi), \text{ (control boundary } \Gamma_c) \tag{54}$$
$$\theta = \theta_s, \quad \text{for } 0 \le r \le R_c, z = H, \tag{55}$$
$$\theta = \theta_s + \frac{r - R_c}{R - R_c}(\theta_t - \theta_s), \quad \text{for } R_c \le r \le R, z = H, \tag{56}$$
$$\theta = \theta_t, \quad \text{for } 0 \le r \le R, z = 0. \tag{57}$$

For $t = 0$ we start with a given temperature profile $\theta_c = \theta_{c0}$ on Γ_c and with $\theta_t = 1690\,K$, $\theta_b = 1708\,K$ for θ_{c0} we have

$$\theta_{c0}(z) = \theta_b + \frac{z}{H}(\theta_t - \theta_b)\ .$$

The velocity field $\overline{\boldsymbol{u}}$, which we want to approach, is a typical toroidal steady twodimensional velocity field. The figure 2 shows the temperature θ_c on Γ_{cT} as the result of the optimization over 60 time steps (= 48,4 seconds). In figure 3 the linear profile $\theta_c(0) = \theta_0$ at the time $t = 0$ and the profile $\theta_c(T)$ are plotted. The figure 4 shows the development of the functional value during the iteration (regularization parameter $\alpha = 0.5$, relaxation parameter $\sigma_r = 0.75$). The figure 4 shows the fast convergence of the fixpoint iteration with relaxation, and these results are better than the results with gradient methods using time step control. As a second testproblem we consider a zone melting configuration. In the table 2 the used geometrical and material parameters for the crystal $(Bi_{0.25}Sb_{0.75})_2Te_2$, a composition of bismuth point fifty antimony one point fifty telurium two, are summarized ([1]).

parameter	symbol	value
radius of the ampulla	R	0.004 m
height of the melt	H	0.016 m
melting point temperatur	θ_s	613 K
thermal diffusivity	a	0.44000e-05 $\frac{m^2}{s}$
kinematic viscosity	ν	0.36310e-06 $\frac{m^2}{s}$
thermal expansion coefficient	β	0.96000e-04 K^{-1}

Table 2. Parameters of $(Bi_{0.25}Sb_{0.75})_2Te_2$-melt and of the melt geometry

$(Bi_{0.25}Sb_{0.75})_2Te_2$-crystals are used for small cooling devices. The figure 5 shows the physical domain of the melt zone. For the velocity we have homogeneous dirichlet data on the whole boundary. For the temperature we have the boundary conditions

$$\theta = \theta_c \quad \text{for } r = R, 0 \le z \le H, \varphi \in (0, 2\pi), \text{ (control boundary } \Gamma_c) \tag{58}$$

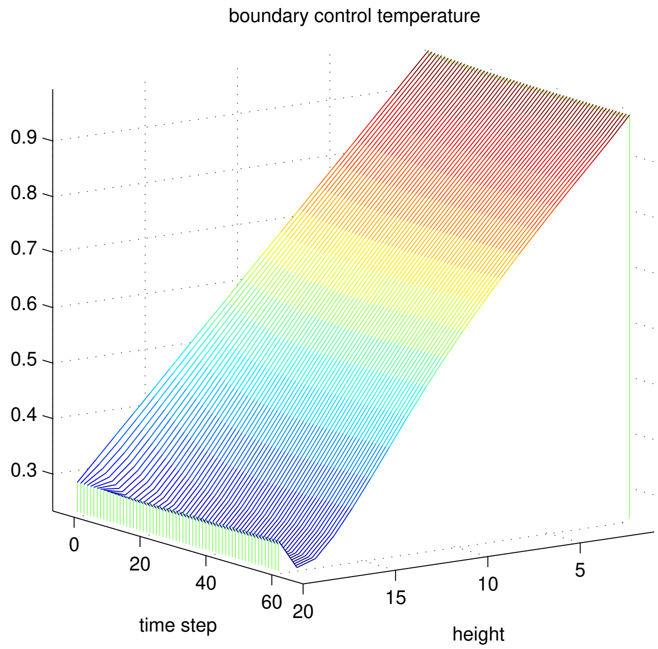

Fig. 2. control on the boundary time cylinder

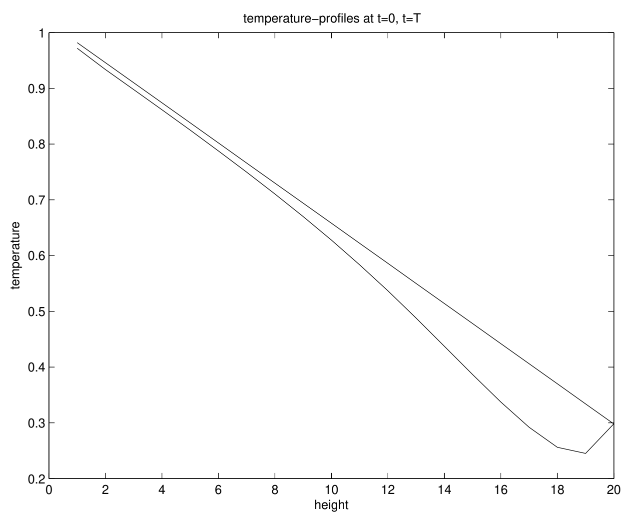

Fig. 3. control θ_c at $t = 0$ and $t = T$

$$\theta = \theta_s, \quad \text{for } 0 \le r \le R, z = H, \tag{59}$$

$$\theta = \theta_s, \quad \text{for } 0 \le r \le R, z = 0. \tag{60}$$

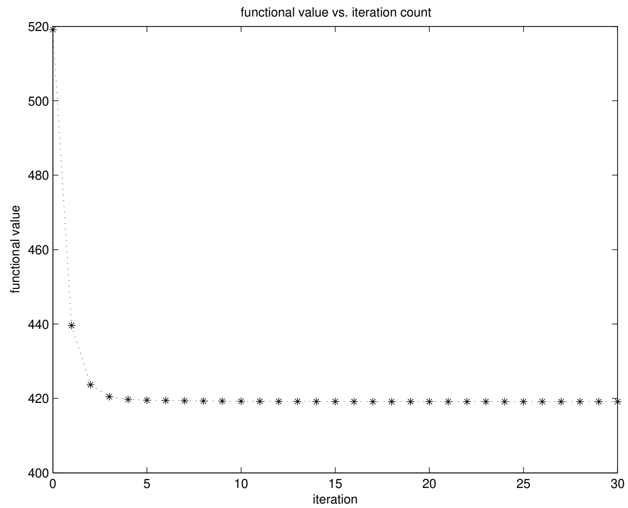

Fig. 4. decreasing functional values during the fixpoint iteration

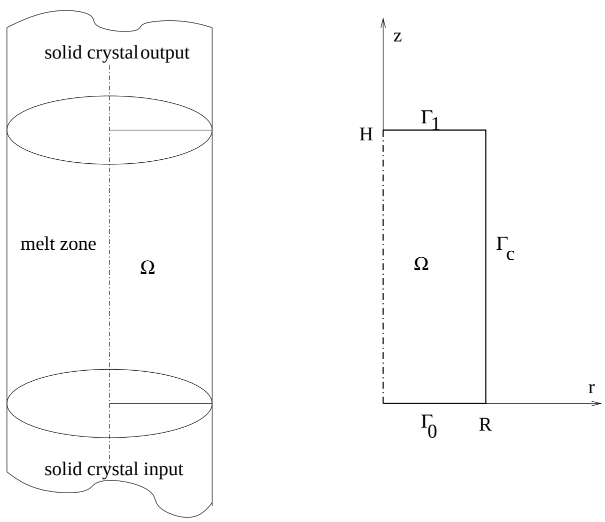

Fig. 5. Physical domain for the zone melting growth

For $t = 0$ we start with a given temperature profile $\theta_c = \theta_{c0}$ on Γ_c and with $\theta_s = 613\,K$, $\delta\theta = 25\,K$ for θ_{c0} we have

$$\theta_{c0}(z) = \theta_s + 4\frac{z}{H}(1 - \frac{z}{H})\delta\theta \ .$$

The velocity field $\overline{\boldsymbol{u}}$, which we want to reach is

i) a typical twodimensional toroidal flow and
ii) a non moving melt $\overline{\boldsymbol{u}} = \mathbf{0}$.

The case ii) is artificial but a good test case because we knew that $\theta_c = \theta_s = const.$ gives $\boldsymbol{u} = \mathbf{0}$ and $\theta = \theta_s$ as a solution of the boussinesq equation system. Artificial means that $\theta = \theta_s$ on Ω is not realistic for a crystal melt and the input mixed crystal will never change to a single homogeneous output crystal. We consider a time interval $[0, T] = [0, 4\,\text{seconds}]$ with $Z = 60$ time steps of 0.0661 seconds. For the given problems we use the optimization system (I). For the spatial discretization we use 20×25 finite volumes. The figures 6 and 7 show the result of the optimization for the case i) and the figures 8 and 9 the result for the case ii).

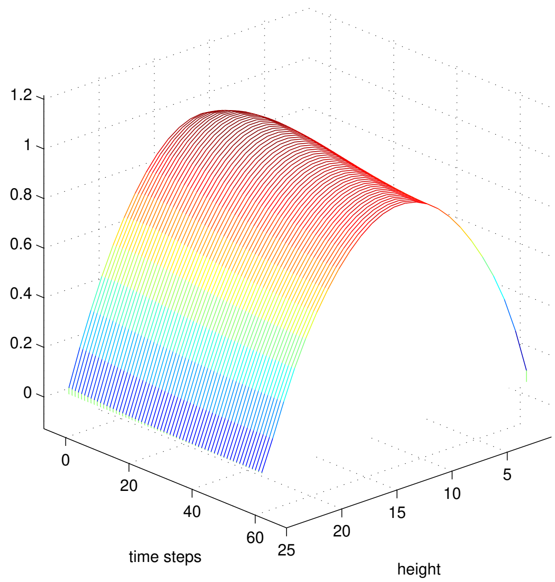

Fig. 6. control on the boundary time cylinder

7 Thermal boundary conditions of third and second order

The heating of the crystal melt is normally realized by a heat source around the crucible or the ampulla, for example by an inductor. This leads to boundary condition of the form

$$\lambda \frac{\partial \theta}{\partial \mathbf{n}} + \tilde{a}(\theta - \theta_0) = \tilde{q} \quad \text{on} \quad \Gamma_{cT}, \tag{61}$$

where q is the normal component of a given heat flux vector and θ_0 is a given environmental temperature. We can write the thermal boundary condition (62) as

$$a \frac{\partial \theta}{\partial \mathbf{n}} + b\theta = q \quad \text{on} \quad \Gamma_{cT}, \tag{62}$$

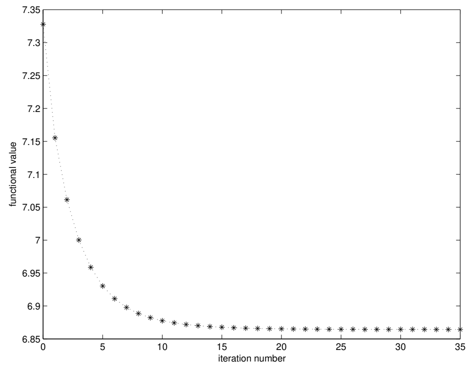

Fig. 7. decreasing functional values during the fixpoint iteration

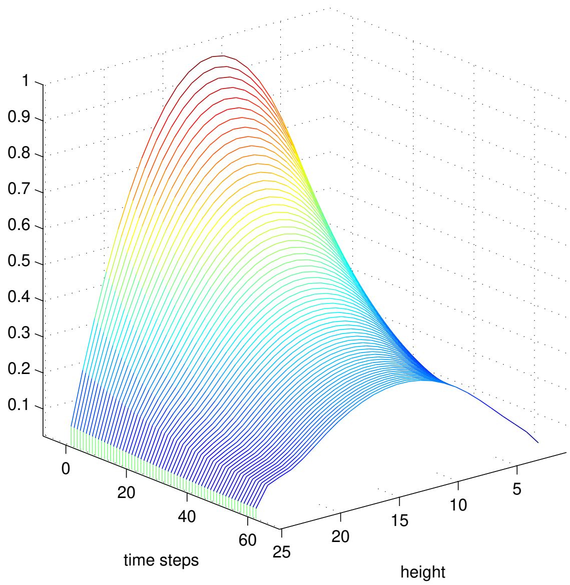

Fig. 8. control on the boundary time cylinder

with given coefficients a, b which are different from zero and the control q. This leads to a modification of the functional

$$J(\boldsymbol{u}, q) = \frac{1}{2}\int_0^T \int_\Omega |\boldsymbol{u} - \overline{\boldsymbol{u}}|^2 \, d\Omega dt + \frac{\alpha}{2}\int_0^T \int_{\Gamma_c} (q^2 + q_t^2) \, d\Omega dt \tag{63}$$

and the Lagrange functional

$$\begin{aligned} L(\boldsymbol{u}, p, \theta, q, \boldsymbol{\mu}, \xi, \kappa, \chi) &= J(\boldsymbol{u}, q) + < \boldsymbol{\mu}, mo >_{\Omega_T} \\ - < \xi, div\, \boldsymbol{u} >_{\Omega_T} &+ < \kappa, en >_{\Omega_T} + < \chi, a\frac{\partial \theta}{\partial \mathbf{n}} + b\theta - q >_{\Gamma_{cT}} . \end{aligned} \tag{64}$$

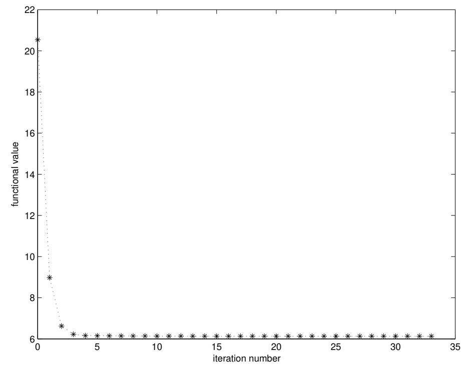

Fig. 9. decreasing functional values during the fixpoint iteration

Using the boundary condition (62) for $L_\theta\tilde\theta$ we get

$$L_\theta\tilde\theta =< -Gr\,\boldsymbol{g}\,\tilde\theta, \boldsymbol{\mu} >_{\Omega_T} + < \kappa, en_\theta >_{\Omega_T} + < \chi, a\frac{\partial\tilde\theta}{\partial\mathbf{n}} + b\tilde\theta >_{\Gamma_{cT}} = 0\ . \quad (65)$$

The evaluation of $< \kappa, en_\theta >_{\Omega_T}$ leads to the same equation as above

$$-\kappa_t - \frac{1}{Pr}\Delta\kappa - (\boldsymbol{u}\cdot\nabla)\kappa = Gr\,\boldsymbol{g}\cdot\boldsymbol{\mu} \quad \text{in} \quad \Omega_T\ , \quad (66)$$

but on the control boundary Γ_c we have to use the boundary condition

$$a\frac{\partial\kappa}{\partial\mathbf{n}} + b\kappa = 0\ . \quad (67)$$

The choice of this boundary condition is necessary to compense the boundary integrals of $< \chi, a\frac{\partial\tilde\theta}{\partial\mathbf{n}} + b\tilde\theta >_{\Gamma_{cT}}$ by the boundary integrals, which we get during the integration by parts of $< \kappa, en_\theta >_{\Omega_T}$. We get the sum of boundary integrals

$$-\frac{1}{Pr}\int_{\Gamma_{cT}}\frac{\partial\tilde\theta}{\partial\mathbf{n}}\kappa\, d\Gamma dt + \frac{1}{Pr}\int_{\Gamma_{cT}}\frac{\partial\kappa}{\partial\mathbf{n}}\tilde\theta\, d\Gamma dt + a\int_{\Gamma_{cT}}\frac{\partial\tilde\theta}{\partial\mathbf{n}}\chi\, d\Gamma dt + b\int_{\Gamma_{cT}}\tilde\theta\chi\, d\Gamma dt\ , \quad (68)$$

and with the choice of χ as

$$\chi = -\frac{1}{b\,Pr}\frac{\partial\kappa}{\partial\mathbf{n}}$$

the second and the fourth part of the sum (68) vanish. With the choice of the boundary condition (67) the first and the third part of the sum (68) vanish.
On the other boundary $\Gamma\setminus\Gamma_c$ we have the boundary condition $\kappa = 0$. For the control q we get the two point boundary value problem

$$\alpha(-q_{tt} + q) = \chi\ (= -\frac{1}{b\,Pr}\frac{\partial\kappa}{\partial\mathbf{n}}) \quad \text{on} \quad \Gamma_{cT}\ , \quad (69)$$

with the time boundary conditions

$$q(0) = q_0 \quad \text{and} \quad q_t(T) = 0\ . \quad (70)$$

If b is equal to zero (62) becomes to

$$a\frac{\partial \theta}{\partial \mathbf{n}} = q \tag{71}$$

and this makes the choice

$$\chi = \frac{1}{a\,Pr}\kappa$$

necessary with the boundary condition

$$\frac{\partial \kappa}{\partial \mathbf{n}} = 0 \tag{72}$$

for the adjoint temperature κ. All other part of the above discussed optimization system will not change.

As a testproblem for thermal boundary conditions of third and second order we use the above discussed zone melting example. Instead of the control boundary condition (58) we use

$$a\frac{\partial \theta}{\partial \mathbf{n}} = q \quad \text{for } r = R, 0 \leq z \leq H, \varphi \in (0, 2\pi), \text{ (control boundary } \Gamma_c) \;, \tag{73}$$

and for the adjoint temperature κ we have on Γ_c the boundary condition

$$\frac{\partial \kappa}{\partial \mathbf{n}} = 0 \quad \text{for } r = R, 0 \leq z \leq H, \varphi \in (0, 2\pi), \;, \tag{74}$$

to consider. We try to reach a typical toroidal melt flow (above discussed zone melting problem i)) by a control q during the boundary condition (73). We start with $a = \lambda = 8,5\,\frac{W}{mK}$, $q = q_0 = 13000\,\frac{W}{m^2}$ and the above noted geometrical and material parameters of the mixed crystal $(Bi_{0.25}Sb_{0.75})_2Te_2$. The figure 10 shows the convergence history of the optimization iteration. The optimal q over the ampulla height and time (on Γ_{cT}) is shown in figure 11.

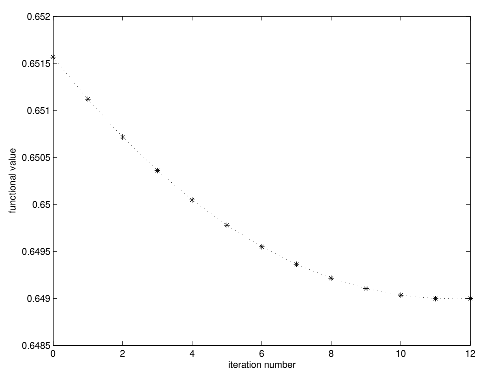

Fig. 10. decreasing functional values during the fixpoint iteration

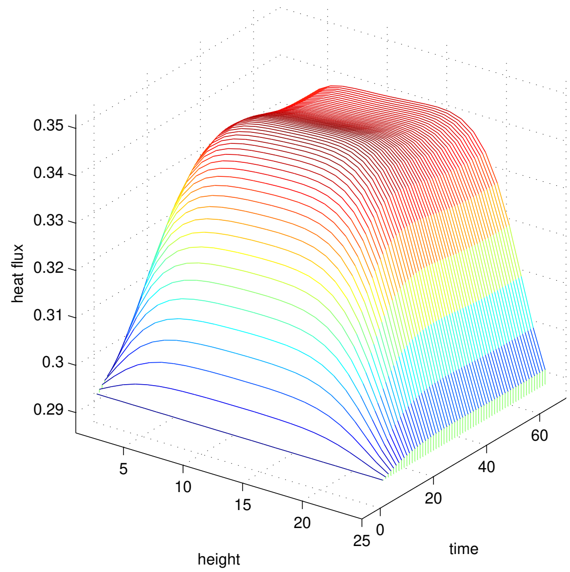

Fig. 11. control on the boundary time cylinder

8 Instantaneous control

The basic idea of the instantaneous control is the time stepwise optimization instead of the optimization over the whol time interval $[0, T]$. The starting point for the instantaneous or suboptimal control is a time discretization of the Boussinesqu equation system, i.e. in the case of an Euler backward ($\sigma_m = \sigma_h = 0$) time discretization with the time step parameter τ

$$\boldsymbol{u} - \tau \Delta \boldsymbol{u} + \tau \nabla p = \tau Gr\, \theta\, \boldsymbol{g} - \tau(\boldsymbol{u}^o \cdot \nabla)\boldsymbol{u}^o + \boldsymbol{u}^o \ , \quad -div\, \boldsymbol{u} = 0 \quad \text{in} \quad \Omega, \tag{75}$$

$$\boldsymbol{u} = \boldsymbol{0} \quad \text{on} \quad \Gamma, \tag{76}$$

where the upper index o means the values at the actual time level. Quantities without an index are considered at the new time level. The Euler backward time discretization of the heat conduction equation leads to

$$\theta - \tau \frac{1}{Pr} \Delta \theta = -\tau(\boldsymbol{u}^o \cdot \nabla)\theta^o + \theta^o \quad \text{in} \quad \Omega, \tag{77}$$

$$\theta = \theta_s \quad \text{on} \quad \Gamma_c, \qquad \theta = \theta_d \quad \text{on} \quad \Gamma_d \ . \tag{78}$$

Now we look for a control θ_s, which minimizes the functional

$$J_s(\boldsymbol{u}, \theta_s) := \frac{\alpha}{2} \int_{\Gamma_c} \theta_s^2 \, d\Gamma + \frac{1}{2} \int_{\Omega} |\boldsymbol{u} - \overline{\boldsymbol{u}}|^2 \, d\Omega \ . \tag{79}$$

With $\hat{J}_s(\theta_s) := J_s(\boldsymbol{u}(\theta_s), \theta_s) = min!$ for $\boldsymbol{u}$ as a solution of the boundary value problem (75)-(78) for a control θ_s we have a stationary optimization problem per time step and with a sequence of such problems we will get an instantaneous control θ_s over the time period $[0, T]$. The optimality system per time step we get on the same way, which we used in the above discussed time-dependend case. For the adjoint variables $\boldsymbol{\mu}$, ξ. κ and the control θ_s we get for the Lagrange function

$$L(\boldsymbol{u}, p, \theta, \theta_s, \boldsymbol{\mu}, \xi, \kappa, \chi) = J_s(\boldsymbol{u}, \theta_s) + < \boldsymbol{\mu}, mo >_\Omega \\ - < \xi, div\, \boldsymbol{u} >_\Omega + < \kappa, en >_\Omega + < \chi, \theta - \theta_s >_{\Gamma_c} . \tag{80}$$

analyzing the nessecary condition $\nabla L = \mathbf{0}$ the adjoint system

$$\boldsymbol{\mu} - \tau \Delta \boldsymbol{\mu} + \nabla \xi = -(\boldsymbol{u} - \overline{\boldsymbol{u}}) , \quad -\tau div\, \boldsymbol{\mu} = 0 \quad \text{in} \quad \Omega, \tag{81}$$

$$\boldsymbol{\mu} = \mathbf{0} \quad \text{on} \quad \Gamma, \tag{82}$$

$$\kappa - \frac{\tau}{Pr} \Delta \kappa = \tau Gr\, \omega \quad \text{in} \quad \Omega, \tag{83}$$

$$\kappa = 0 \quad \text{on} \quad \Gamma , \tag{84}$$

$$\theta_s = -\frac{\tau}{\alpha Pr} \frac{\partial \kappa}{\partial \mathbf{n}} \quad \text{on} \quad \Gamma_c . \tag{85}$$

The advantage of this technique is obvious, because we have to solve per time step only a small stationary optimization problem. The results of [3] showed the efficiency of the instantaneous control strategy in the case of isothermic flows and it could be shown, that instantaneous controls are very effective compared to optimal controls, i.e. the value of the $\hat{J}(\theta_s)$ was only 10% higher than $\hat{J}(\theta_c)$ in the case of a boundary controlled backward facing step.

9 To the numerical solution method of the instantaneous control problem

The spatial discretization of the equations (75)-(85) will be done with a finite volume method. The solution of the equation (77) gives the temperature field on the new time level. With the choice of

$$\tilde{\boldsymbol{u}} = \boldsymbol{u}^o - \tau (\boldsymbol{u}^o \cdot \nabla) \boldsymbol{u}^o + \tau Gr\, \theta\, \boldsymbol{g} \tag{86}$$

from (75) follwos the equation

$$-\tau \Delta\, p = -div\, \tilde{\boldsymbol{u}} \tag{87}$$

for the pressure on the new time level. With p it is possible to get the velocity field as a solution of

$$\boldsymbol{u} - \tau \Delta \boldsymbol{u} = \tilde{u} - \tau \nabla p . \tag{88}$$

If our wanted velocity field $\bar{\boldsymbol{u}}$ fullfills the condition $div\, \bar{\boldsymbol{u}} = 0$ we can get the adjoint velocity μ as a solution of

$$\boldsymbol{\mu} - \tau \Delta \boldsymbol{\mu} = -(\boldsymbol{u} - \overline{\boldsymbol{u}}) , \tag{89}$$

because the adjoint pressure ξ must be constant. If $div\, \bar{\boldsymbol{u}} \neq 0$ we have to solve a Poisson equation like (87). With $\boldsymbol{\mu}$ we can determine the adjoint temperature field κ and lastly the control θ_s.

10 Conclusion

With the Langrange parameter technique it's possible to derive an optimization system for a given functional, which solution gives an optimal control. The numerical examples of the fully time-depend 2.5d optimization system show the possibility of the practical optimization of a thermal coupled flow problem in the crystal growth field. Based on the results the proposed strategies it is now possible to do a fully 3d optimization.
It is necessary to continue numerical experiments to investigate if the optimization during a boundary control only will be successful technology. There are some experiences with other optimization problems which show the efficiency of volume control, if there is a possibility of the production of volume forces (for example by a magnetic field).
The investigation of thermal boundary condition of third and second order (62),(71) and the heat flux q as a control parameter instead of the boundary temperature will be investigated and the implementation of the instantaneous control is on the table now and the first results are present.
Instantaneous strategies with the used linearizations of (75) and (77) lead to a sequence of time-independend stationary optimization problems, which bring instantaneous results near the optimal control. The instantaneous strategies seem to be a cheap alternative compared to the high resolved fully time-depend optimization.

References

1. Bärwolff, G., König, F. and G. Seifert: Thermal buoyancy convection in vertical zone melting configurations, ZAMM 77 (1997) 10
2. Hinze, M.: Optimal and instantaneous control of the instationary Navier-Stokes equations, habilitation thesis, Berlin, August 2000 (available on the webpage `http:\\www.math.tu-dresden.de\~hinze`)
3. Hinze, M.: Optimization of the Navier-Stokes equation, Adjoints workshop, Decin/Czech Republic, September 2001
4. Ladyzhenskaya, O.: The Mathematical Theory of Viscous Incompressible Flows, Gordon & Breach, 1969
5. Constantin, P. and C. Foias: Navier-Stokes Equations, The University of Chicago Press, 1988
6. Gunzburger, M., Ozugurlu, E., Turner, J. and H. Zhang: Controlling transport phenomena in the Czochralski crystal growth process, Journal of Crystal Growth 234 (2002)
7. Bärwolff, G.: Numerical Modelling of Two- and Three-Dimensional External and Internal Unsteady Incompressible Flow Problems, in: Computational Fluid Dynamics - Selected Topics, D. Leutloff and R.C. Srivastava (Eds.), Springer-Verlag Berlin Heidelberg New York, 1994
8. Böttcher, K.: Collected solid crystal and crystal melt material parameters, Berlin 2003 (available on the webpage `http:www.ikz-berlin.de\~kb`)